Audio Engineering Society

Convention Paper 10311

Presented at the 147th Convention
2019 October 16 – 19, New York

Loudspeaker Port Design for Optimal Performance and Listening Experience

Andri Bezzola[1], Allan Devantier[1], and Elisabeth McMullin[1]

[1]*Samsung Research America, DMS Audio, Valenica CA 91355*

Correspondence should be addressed to Andri Bezzola (andri.b@samsung.com)

ABSTRACT

Bass reflex ports produce noise at high sound-pressure levels due to turbulence and vortex shedding. Flared ports can reduce port noise compared to straight ports, but the optimal flare rate in ports has remained an unsolved problem. This work demonstrates that there is in fact an optimal amount of flare, and it proposes a design method based on acoustic Finite Element simulations to efficiently predict the optimal flare rate for given port dimensions. Optimality of the flare rate is confirmed with noise and compression measurements as well as double-blind listening tests. At onset of unwanted port noise, optimally flared ports can be played 1 to 3 dB louder than slightly under-flared or over-flared ports, and 10 to 16 dB louder than straight ports.

1 Introduction and Literature Review

Bass reflex ports are used to improve the low-frequency performance of loudspeaker systems. The mass of the air in the port combines with the compliance of the air inside the enclosure to create a Helmholtz resonator that reduces cone excursion at port tuning. At low sound pressure levels the air flow in the port remains laminar, extending the frequency response and improving the efficiency of the loudspeaker system. As sound pressure level increases so does the velocity of the air within the port and the flow may become turbulent. Distortion, compression and noise artifacts rise dramatically with the onset of turbulence [1].

Consistently designing a port with minimal noise caused by turbulent flow remains an unsolved problem. Studies based on distortion and compression measurements suggest a gentle flare is best, but previous blind listening tests have confirmed a slightly more flared port is preferred [2]. This work correlates the results of several listening tests to more relevant objective measurements and linear Finite Element Method (FEM) simulations in an effort to find a design methodology that consistently leads to an optimal solution. The solutions are optimal in the sense that optimal ports can play at higher levels (higher port velocities) before flow separation generates unwanted blowing noise.

Backman [3] compared the performance of ten bass reflex ports to a typical straight tube mounted on a baffle. He found that a symmetrical port with a blend at each end and a flange on the inside was optimal. The study also included ports with bends and corners, both of which degraded performance significantly.

Vanderkooy [4, 5] developed the calculations needed to find the tuning frequency for both straight and flared port tubes. He also experimented with ports of various lengths and profiles and demonstrated the chaotic nature of ports operating outside the linear region.

Roozen et al. [6, 7, 8] postulated that boundary layer turbulence and unsteady separation of the acoustic flow are the main causes of noise. From numerical simulations they showed that vortex shedding occurs at the port termination for straight ports and closer to the mid point for a generously flared port. They numerically and empirically demonstrated that vortex shedding creates an impulsive excitation of the port Eigenfrequencies resulting in unwanted noise at the $\lambda/2$ port resonance. They concluded that a port with a gentle flare and small blend radii at the ends is optimal to reduce noise.

Salvatti et al. [1] presented an exhaustive study on the subject and conducted several experiments. They concluded that ports with generous flares performed best at low sound pressure levels and straight ports performed best at extremely high levels. They also suggested that ports with moderate flare represented the best compromise over a wide range of sound pressure levels.

Rapoport and Devantier [2] used Computational Fluid Dynamics (CFD) to model the unsteady flow of the air in the port. They modeled, built, and measured six ports of various flare rates ranging from straight with blend radii to "over-flared". Distortion and compression measurements hinted at an optimal design but blind listening tests contradicted the notion that the port with lowest distortion was preferred by listeners. Subsequent blind listening tests – previously not published – found an optimal solution. This paper will present those results and expand on their work.

More recently, Backman returned to the subject in 2016 [9]. He built a CFD model of a bass reflex loudspeaker system with a straight port and a 160 mm woofer in a 16-liter enclosure. He concluded that the combination of CFD modelling and acoustic-based boundary conditions is capable of describing the qualitative behavior of a ported loudspeaker system. In 2017, he built on his earlier work analyzing the performance of his model over a wide range of sound pressure levels [10]. He was able to model the well-known phenomena of port compression and resonance shift.

In 2017, Garcia-Alcaide et al. [11] published a paper investigating vortex shedding as a source of port noise using numerical and experimental techniques. They observed noise in the 1 kHz region for a port tuned at 65 Hz.

Finally, in 2018 Button et al. [12] characterized the acoustic mass and the acoustic resistance of two different loudspeaker ports as a function of drive level.

The fluid flow in a loudspeaker port can be fully described by the Navier-Stokes (NS) equations. The NS equations describe momentum conservation in fluids, including fully turbulent flow, flow separation etc., but they are notoriously hard to solve. The NS equations can be linearized, and under the assumption of negligible viscosity and thermal conductivity, they can be formulated as the Linear Wave equation in the time domain, or the Helmholtz equation in the frequency domain, which are much easier to solve.

2 Rapoport and Devantier 2004, Revisited

Rapoport and Devantier [2] built and tested six ports with varying flare rates. Port SR was a straight port with blend radii on the ends and a flange on the inside. The remaining five ports were continuously flared. Port A had the least amount of flare and port E had the most. Port C had the least amount of compression and harmonic distortion at high SPLs. Table 1 describes the ports that are relevant to this paper and Figure 1 shows the total harmonic distortion data.

Several blind listening tests were performed on Ports SR, B, C, and D with the hope of showing that Port C was optimal. However, listeners preferred the port with the most flare in the blind tests, port D. An additional blind listening test was run with port E replacing port SR. The listening test was similar to the one described in section 6.1 of [2] except the drive levels were 7, 10, 14, 20 Vrms. In that test, port D was still preferred by listeners as shown in Figure 2. They found that there is an optimal amount of flare. Unfortunately, this listening test was completed after the Fall 2004 AES paper submission deadline and was not reported in the published paper.

Port	**B**	**C**	**D**	**E**
Length [mm]	120	120	120	120
D_c [mm]	62.9	61.8	60.9	60.1
D_e [mm]	79.2	87.4	96.7	107
R_b [mm]	15	15	15	15
V_{box} [L]	24.6	24.6	24.6	24.6

Table 1: Parameters for ports from [2] including extra port E. D_c is inner diameter at center of port, D_e is the inner diameter at exit of port, and R_b is blend radius applied at ends of port.

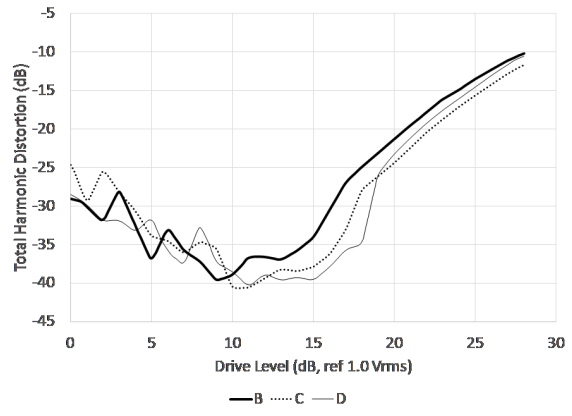

Fig. 1: Total Harmonic Distortion data for ports B, C and D of [2].

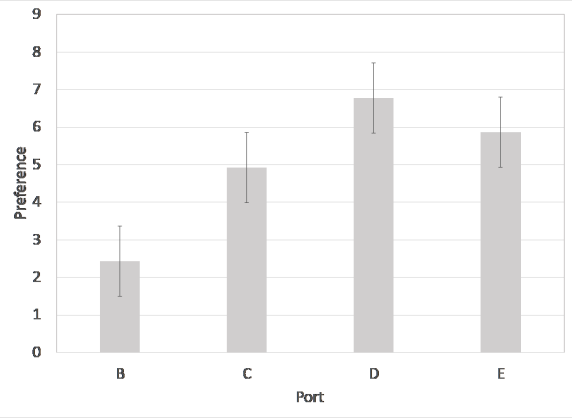

Fig. 2: Results (mean values with 95% confidence intervals) of a blind listening test conducted after the Fall 2004 AES convention submission deadline.

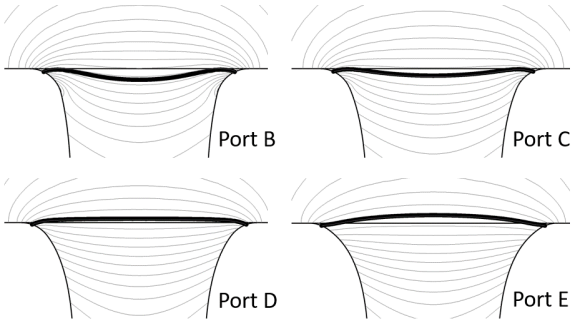

Fig. 3: Particle velocity contour lines for ports B, C, D, and E from [2]. The velocity contours of the best sounding port, D, had the least curvature at the port ends.

3 Acoustic FEM Simulations of Rapoport and Devantier 2004 Ports

The Helmholtz equation was solved for ports B, C, D, and E in COMSOL Multiphysics [13] in an effort to gain some insight without having to solve the numerically expensive NS equations. Solving the acoustic Helmholtz equation at 30 Hz, the port resonance frequency, revealed an interesting phenomenon. The contours of the RMS particle velocity at the ends of port D (the best sounding port) show minimal curvature. Ports with less flare have concave velocity contours and ports with more flare have convex velocity contours at the ends (see Figure 3).

4 Flow Separation and Port Noise

The observation that the optimal port in [2] had minimal curvature in the particle velocity contours correlates well with the equations for flow separation, for which the stream-wise momentum equation can be written as:

$$u\frac{\partial u}{\partial s} = -\frac{dp}{ds} + \nu\frac{\partial^2 u}{\partial y^2} \tag{1}$$

where u is the velocity along stream lines and s, y, are stream-wise and normal coordinates. Flow reversal is primarily caused by an adverse pressure gradient imposed in the boundary layer. An adverse pressure gradient is when shear stress $\frac{dp}{ds} > 0$, which can be seen to cause the velocity u to decrease along s and possibly go to zero if the adverse pressure gradient is strong enough as illustrated in Figure 4.

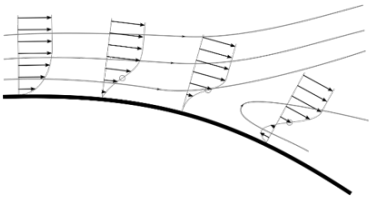

Fig. 4: Graphical representation of the velocity profile in the boundary layer. The last profile represents adverse pressure gradient which results in separated flow. Continuous lines are streamlines and arrows are local velocity vectors. By Olivier Cleynen, licensed by CC BY 3.0.

While equation (1) is typically used for flow separation in unidirectional flow in boundary layers, it offers a possible insight into how to optimize loudspeaker port tubes with bidirectional flow. Several studies have focused on turbulence in ports [1, 2, 3, 10], and some have focused on flow separation as the source of unwanted port noise [6, 7, 8, 11]. Flow separation leads to vortex shedding, which can excite the air inside the port tubes with an impulse-like disturbance. This impulse excites all frequencies in the port, and most critically, it will excite the Eigenfrequency of the air inside the port. Disregarding end corrections, the first Eigenfrequency of ports f_p^1 can be estimated by the half-wavelength

$$f_p^1 \approx \frac{c}{2L}, \tag{2}$$

where c is the speed of sound, and L is the nominal port length.

For typical port lengths in bass reflex boxes below 0.5 m, f_p^1 is larger than 343 Hz, which is several octaves higher than the port tuning frequency. When the port Eigenfrequencies get excited by flow separation and vortex shedding, they are very audible to the human ear, because they are outside the spectral masking bandwidth of the nominal port operating frequencies. The unwanted "noise" that is associated with the port Eigenfrequencies is often interpreted as turbulent air noise in ports. The word "noise" in this context is not related to a random signal like measurement noise, but rather expresses the unwanted audible high-frequency content from a port that is driven at high levels.

5 New Hypothesis

Based on the observation that the best sounding port in [2] had the least amount of shear rate, combined with the presented argument that vortex shedding produces audible port "noise," the following hypothesis was made:

> "The best sounding port has the lowest propensity for flow separation. Flow separation is minimal when the particle velocity contours at port exit have minimal curvature."

To test this hypothesis, eight more ports were designed and tested with different ratios of length to central diameter.

6 Acoustic FEM Simulations of Ports with Different Aspect Ratios

All the ports in [2] were 120-mm long and the minimum diameter was nominally 60 mm. Therefore, the aspect ratio of the ports was approximately 2:1. To test the hypothesis, ports with an aspect ratio of 3:1 and 4:1 were designed.

In order to find the optimal port profile, the following iterative method was used.

1. Fix central diameter (D_c) at 59 mm.
2. Find box volume (V_{box}) to keep port tuning frequency at 40 Hz.
3. Optimize exit diameter (D_e) and blend radius (R_b) until minimal curvature is observed in the velocity contours at port exit.
4. Repeat steps 2 and 3 until convergence is found.

After finding the optimal port for each aspect ratio, four more ports were designed with central diameters of 57 mm and 61 mm for each aspect ratio. The blend radius and box volume was kept fixed for all ports with the same aspect ratio, but the flare rate was adjusted to result in a port tuning of 40 Hz for all ports. For the 3:1 aspect ratio, two additional ports were prototyped: a traditional straight port, and a straight port with blends and flanges at the port exits.

The parameters of all the tested ports are listed in Table 2. The particle velocity contours resulting from the acoustic FEM simulations are shown in Figure 5 for the 3:1 aspect ratio ports and in Figure 6 for the 4:1 aspect ratio ports. Additional details on the implementation in COMSOL can be found in [14].

Port	**57 mm**	**59 mm**	**61 mm**	**Straight w/ blends**	**Straight no blends**	**57 mm**	**59 mm**	**61 mm**
Aspect Ratio	3:1	3:1	3:1	3:1	3:1	4:1	4:1	4:1
Length [mm]	180	180	180	180	180	240	240	240
D_c [mm]	57	59	61	69	69	57	59	61
D_e [mm]	177	117	97	69	69	150	126	102
R_b [mm]	8.4	8.4	8.4	8.4	-	10.1	10.1	10.1
V_{box} [L]	30.6	30.6	30.6	30.6	30.6	24.6	24.6	24.6

Table 2: Parameters for ports with 3:1 and 4:1 aspect ratio.

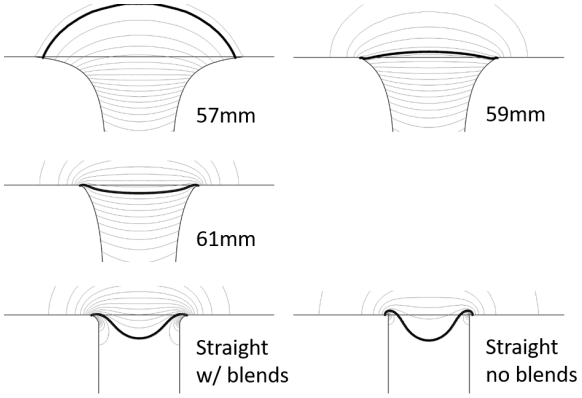

Fig. 5: Particle velocity contours for ports with 3:1 aspect ratio at port tuning frequency of 40 Hz.

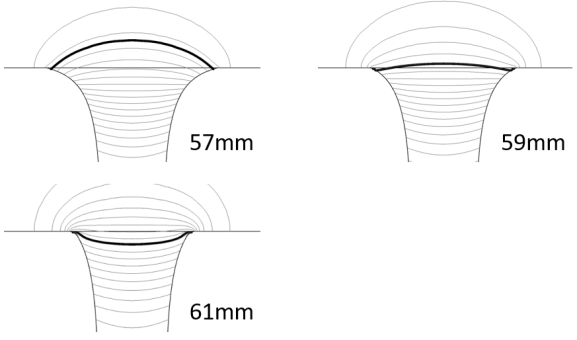

Fig. 6: Velocity contour plots of the ports with 4:1 aspect ratio at port tuning frequency of 40 Hz

Fig. 7: Photos of test box with two 10-inch woofers and microphone fixture. Left: Box before mounting. Middle: Box with port mounted inside hemi-anechoic chamber. Left: Box mounted to hemi-anechoic chamber wall, shown from outside.

7 Port Measurements

7.1 Port Noise Measurements

In order to measure port noise, two medium density fiberboard boxes were constructed with a baffle to mount the box in a hemi-anechoic (2π) chamber. A GRAS microphone fixture was mounted on the baffle to hold a G.R.A.S. 46 AM microphone, angled 45° at a distance of 10 cm from the port exits. Two 4 Ω 10-inch subwoofer drivers were mounted in opposing sides of the boxes. This solution provides force-cancellation, where the drivers' forces oppose each other, and the drivers' axes are parallel to the mounting surface on the 2π chamber wall. This configuration puts minimal force perpendicular to the mounting surface, ensuring low distortion from motion of the baffle and mounting surface. The test box setup is shown in Figure 7.

The woofers were driven by a QSC RMX 5050a amplifier with 1600 W/channel at 4 Ω. The test signal for the ports with aspect ratio of 3:1 was a series of 16 x 250 ms long multitone signal with a bandwidth

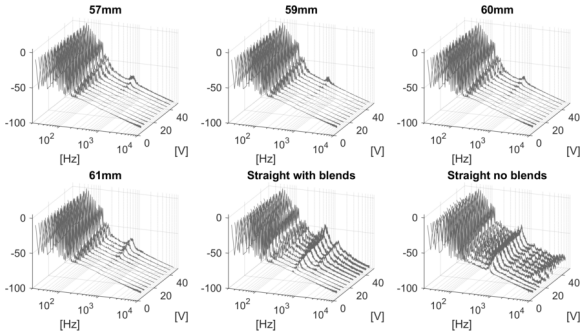

Fig. 8: Normalized spectra for ports with 3:1 aspect ratio at different voltage levels.

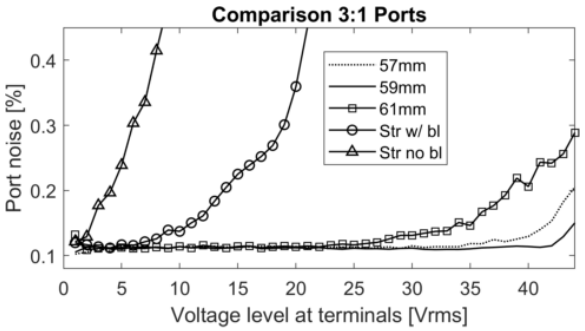

Fig. 9: Port noise for ports with 3:1 aspect ratio. Noise measured as ratio of spectral content in octave around f_p^1 to total spectral content at different drive levels.

of 20 Hz to 160 Hz [15]. The 16 repetitions were averaged to reduce the measurement noise. The voltage at the speaker terminals was stepped up from 1 Vrms to 44 Vrms. Beyond 44 Vrms the amplifier started to clip the output signal. The results for the 3:1 aspect ratio ports are shown in Figure 8. The plots clearly show how port "noise" around $f_p^1 \approx 950$ Hz develops at higher voltages.

A figure of merit for port noise is the amount of spectral content at a bandwidth of one octave around f_p^1, compared to the total spectral content. The noise levels are plotted in Figure 9. The results clearly show the benefits of rounding the port exits and putting a flange on the end as reported repeatedly [1, 3, 6]. The results also indicate that there is an optimal amount of flare. Too little or too much flare does increases spectral content around f_p^1, as shown by the ports 61 mm or 57 mm respectively.

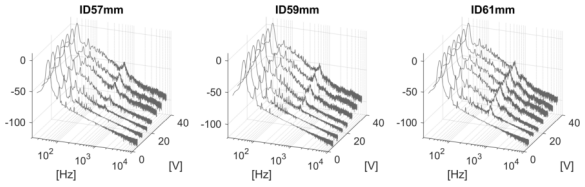

Fig. 10: Normalized spectra for ports with 4:1 aspect ratio at different voltage levels.

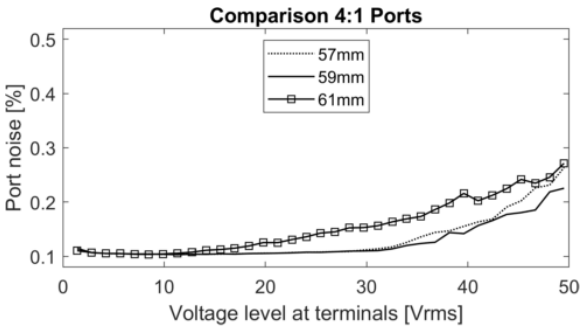

Fig. 11: Port noise for ports with 4:1 aspect ratio. Noise measured as ratio of spectral content in octave around f_p^1 to total spectral content at different drive levels.

When using the same multitone signal with the 4:1 ports that was used in the 3:1 ports, no significant increase in port noise could be detected before amplifier clipping. In order to increase port output, a lower crest factor was required. Therefore, a single sine tone at 40 Hz was used as input signal, with a crest factor of 3 dB. No averaging was done to improve the signal-to-noise ratio for this measurement. The normalized output spectra are shown in Figure 10. The noise peak around $f_p^1 \approx 715$ Hz is clearly noticeable at higher voltage levels. The port noise figure of merit plots are shown in Figure 11. In summary, the noise measurements confirmed the hypothesis that there exists an optimal amount of flare rate in ports. Over-flared and under-flared ports generate more output around the first Eigenfrequency of the port f_p^1. Furthermore, the voltage level with measurable increase of noise around f_p^1 is highest for the ports with optimal flare rate.

7.2 Compression Measurements

In addition to measuring port noise, it is interesting to measure port compression. For this test, a 500-ms long sine burst tone of 40 Hz was used as a stimulus.

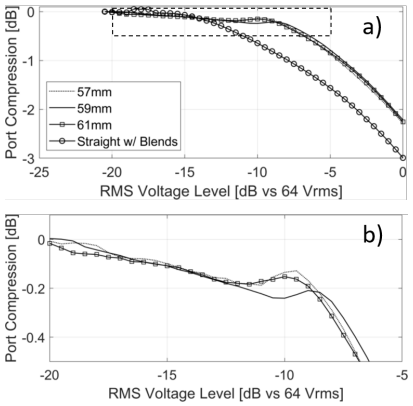

Fig. 12: Compression measurements of ports with 3:1 aspect ratio. a) Straight ports compress at lower drive levels than flared ports. b) close up of dashed area for flared ports reveals compression reversal, before compression acceleration.

The maximum voltage level before amplifier clipping with this signal was 64 Vrms. The measurement was conducted with 0.5-dB increments from -20 dB to 0 dB with respect to 64 Vrms. Subsequent sine bursts were taken in intervals of 10 s in order to minimize any bias associated with thermal compression of the transducers. The port output was measured in the far field at 30° off-axis and 1.8-m distance from the port exit.

The results for 3:1 aspect ratio ports are shown in Figure 12a. Unsurprisingly, the straight port starts to compress at voltage levels several dB lower than the three flared ports. Closer inspection of the compression data of the flared ports (Figure 12b), revealed that there is a voltage level where compression is reversed. As stipulated in [1], it is assumed that this is due to the onset of turbulence and the air-bearing effect. At higher levels full flow separation and vortex shedding occurs and compression is accelerated.

The 59-mm port has the highest drive level at which compression reversal and subsequent acceleration occurs (-10.5 dB), which confirms that it has optimal flare rate and it can play 1 dB louder than 61- and 57-mm ports before the flow becomes turbulent.

8 Listening Tests

Three listening tests were run to validate the results of the port tube simulations and correlate with the measurements. Fifteen listeners participated in two tests with 3:1 aspect ratio ports. Seven listeners participated in one test with 4:1 aspect ratio ports. Listeners ranged in age from 25 to 61 (mean=40, SD=12) and three were female while 12 were male. All listeners were measured for normal audiometric hearing. Twelve of the listeners were considered trained listeners based on their performance from previous experiments.

The tests were administered using custom software made in Max 8, which automated the testing process and results storage. Audio was played back on MrSpeakers Aeon Flow closed-back circumaural headphones which were selected for their low distortion, clean bass performance, and low coloration. Playback level was set for 85 dB when -18 LUFs pink noise was playing back over the headphones on a GRAS KEMAR head fitted with RA0045-S1 ear simulators.

8.1 Preference Test

During the initial round of testing, listeners rated their preference for recordings of the five port tubes. All five port tubes were evaluated during each trial of the test. At the beginning of each trial, the software randomized the playback order of the ports and which of the four voltage levels (4 V, 20 V, 40 V, 60 V) and three tracks (whale drum, kick drum, electric bass guitar) were presented. There were two repeats of each combination of factors for a total of 24 trials. Listeners were instructed to pay particular attention to the distortion and noise artifacts, bass extension, and transparency of each recording. They were then asked to give each a preference rating on a continuous scale from 0 to 100 (Strongly Dislike – Strongly Like) and were each given the option of leaving comments.

Observing the results from test one, there was a clear trend for listeners to prefer the 59-mm port tube at the higher voltages, particularly 40 V. Across all playback voltages the straight port tube received low ratings and the straight blended port tube received low ratings at voltages above 4 V. The results of test round one were evaluated using a factorial ANOVA with repeated measures considering port (N=5), voltage (N=4), track (N=3), and observation (N=2) as fixed factors.

The results indicated the following significant effects: port ($F(4,64)=3.90$, $p<0.01$), voltage ($F(1.22,19.58)=266.22$, $p<0.001$), and track ($F(2,32)=73.64$, $p<0.001$). Pairwise comparisons with a Bonferroni correction were run on all the fixed factors

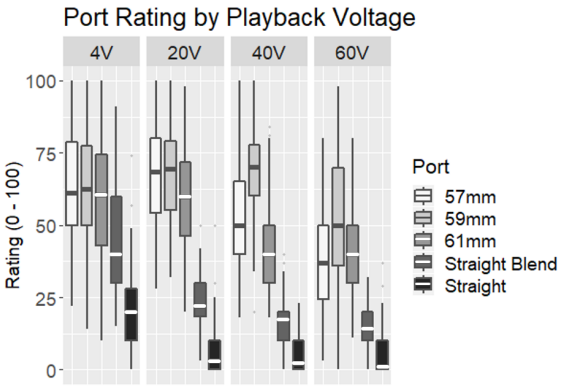

Fig. 13: Overall port ratings by playback level for the preference test.

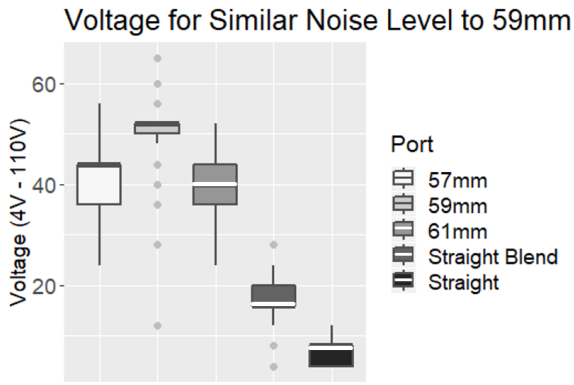

Fig. 14: Results of MoA test with 3:1 aspect ratio ports. Selected levels at which port noise was equal to the noise of port 59 mm at 52 Vrms.

and showed that all five ports received significantly different ratings, a playback voltage of 20 V and 40 V gave similar ratings, and the bass drum track received significantly higher ratings than the other two tracks. Unsurprisingly, there were also significant interactions by voltage by port ($F(3.56, 192)=14.63$, $p<0.001$), by voltage by track ($F(3.67,96)=25.73$, $p<0.001$), and by track by port ($F(2.48,128)=14.83$, $p<0.001$).

A summary of the findings is shown in Figure 13 where the results by port and by voltage are shown. There are striking correlations between the port noise measurements and the listening test results. Both the listening tests and measurements show that the flared ports significantly outperform the straight ports even at low levels. Focusing on the 57-mm and 61-mm ports, it becomes evident that the port performances are compromised at and above 40 volts. The 59 mm performed well even at 40 volts, and only at 60 volts was a performance degradation observed.

8.2 Method of Adjustment Test

During test session two, listeners used a method of adjustment (MoA) procedure to select a playback voltage which had the same amount of noise and distortion artifacts as a reference port tube recording. The audio stimulus used to make the recording was a sample of a whale drum which was used in the previous round of testing. The playback levels of the recordings at different voltages were loudness normalized by input voltage. The reference port tube recording for the 3:1 aspect ratio ports was of the 59 mm port played back at 52 V. This voltage was selected as a point in which the 59 mm port started to generate a small but discernible amount of noise. At the beginning of each trial, the software selected a port and initial playback voltage and listeners turned a rotary encoder knob up or down to play back the port recorded at a higher or lower voltage. They could toggle the reference signal on or off for comparison at any time. There were 25 possible playback voltages which ranged from 4 V to 110 V. The steps between voltages were 4 V up until 60 V and 5 V above that point. Each port was played five times to account for repeatability.

The results of the 3:1 MoA test demonstrated that the 59-mm port was significantly less noisy and required at least 8 V more level (based on the difference in medians) to produce a similar amount of noise when compared to the 57 and 61 mm ports. Overall, listeners were very consistent in picking out the reference port voltage level in this experiment, indicating that the listener sample performed well and the task was relatively easy. Listeners tended to rate the required voltage levels similarly for the 57-mm and 61-mm ports (between 36 V and 44 V, i.e.: between 3.2 dB and 1.5 dB less) demonstrating that they were noisy at similar levels. The noise performance of the straight port and straight blended port was quite poor, requiring only 8 V and 16 V respectively (i.e.: 16.3 dB and 10.2 dB less) to have a similar levels of noise with the 59 mm at 52 V. The results of the MoA test with 3:1 aspect ratio ports are shown in Figure 14.

A similar MoA test was run with three 4:1 aspect ratio ports. For this test, seven participants listened to a

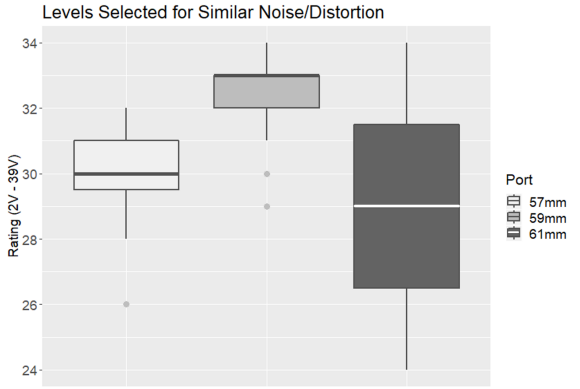

Fig. 15: Results of MoA test with 4:1 aspect ratio ports. Selected levels at which port noise was equal to the noise of port 59 mm at 33 V.

half-second loudness-normalized sine burst. The reference recording was of the 59 mm port at 33 V. The selectable voltages for this test ranged from 1 V to 40 V in 1 V steps, and each port was played five times in randomized order with randomized initial voltage levels.

The results of the 4:1 MoA test in Figure 15 demonstrated that the 59-mm port could play 3 V (0.8 dB) louder than the 57- mm port before noise was equally noticeable. On average, port 61 mm needed to be played 4 V (1.1 dB) less loud to match the noise level of the 59 mm port, but the port had an unusually a wide distribution. It is suspected that the wide distribution stems from the fact that the 61-mm port had additional audible distortion that was not related to blowing noises, which could have influenced the listeners. Again, listeners were very consistent in picking out the reference port level.

In summary an optimal port can play 0.8 to 3 dB louder before noise becomes audible compared to slightly over-flared or under-flared ports respectively. An optimal port can play 10 to 16 dB louder before noise becomes audible, compared to straight ports.

9 Conclusion

This work demonstrates that there is an optimal amount of flare rate for bass reflex ports. More or less flare results in ports that perform worse in noise and compression measurements and also perform worse in listening tests. For ports with nominal diameter of 60 mm, a 2-mm (3.3%) change in central diameter resulted in performance hit of 0.8 to 3 dB. Straight ports performed 10 to 16 dB worse than optimally flared ports.

This work also shows how optimal port profiles can be designed very efficiently by method of linear acoustic FEM simulations and observation of the particle velocity contours at port exit, rather than solving the turbulent flow with numerically expensive CFD simulations. A flat particle velocity contour correlates with optimal performance measurements and listening experience.

Samsung Electronics and Samsung Research America supported this work. The authors would like to thank the entire staff of Samsung's US Audio Lab who helped with all aspects of this research, offered insightful suggestions, and contributed to this work.

References

[1] Salvatti, A., Devantier, A., and Button, D. J., "Maximizing performance from loudspeaker ports," *Journal of the Audio Engineering Society*, 50(1-2), pp. 19–45, 2002, ISSN 0004-7554.

[2] Rapoport, Z. and Devantier, A., "Analysis and Modeling of the Bi-Directional Fluid Flow in Loudspeaker Ports," in *Audio Engineering Society Convention 117*, San Francisco, 2004.

[3] Backman, J., "The nonlinear behavior of reflex ports," in *Audio Engineering Society Convention 98*, Paris, 1995.

[4] Vanderkooy, J., "Loudspeaker Ports," in *Audio Engineering Society Convention 103*, New York City, 1997.

[5] Vanderkooy, J., "Nonlinearities in Loudspeaker Ports," in *Audio Engineering Society Convention 104*, Amsterdam, 1998.

[6] Roozen, N. B., Bockholts, M., van Eck, P., and Hirschberg, A., "Vortex sound in bass-reflex ports of loudspeakers. Part I. Observation of response to harmonic excitation and remedial measures," *The Journal of the Acoustical Society of America*, 104(4), pp. 1914–1918, 1998, ISSN 0001-4966, doi:10.1121/1.423760.

[7] Roozen, N. B., Bockholts, M., van Eck, P., and Hirschberg, A., "Vortex sound in bass-reflex ports of loudspeakers. Part II. A method to estimate the point of separation," *The Journal of the Acoustical Society of America*, 104(4), pp. 1919–1924, 1998, ISSN 0001-4966, doi:10.1121/1.423762.

[8] Roozen, N. B., Vael, J. E. M., and Nieuwendijk, J. A., "Reduction of Bass-Reflex Port Nonlinearities by Optimizing the Port Geometry," in *Audio Engineering Society Convention 104*, Amsterdam, 1998.

[9] Backman, J., "Fluid dynamics analysis of ported loudspeakers," in *Audio Engineering Society Convention 141*, Los Angeles, 2016.

[10] Backman, J., "Nonlinearity of ported louspeaker enclosures," in *Audio Engineering Society Convention 142*, Berlin, 2017.

[11] Garcia-Alcaide, V. M., Palleja-Cabre, S., Castilla, R., Gamez-Montero, P. J., Romeu, J., Pamies, T., Amate, J., and Milan, N., "Numerical study of the aerodynamics of sound sources in a bass-reflex port," *Engineering Applications of Computational Fluid Mechanics*, 11(1), pp. 210–224, 2017, ISSN 1997003X, doi:10.1080/19942060.2016.1277166.

[12] Button, D., Lambert, R., Brunet, P., and Bunning, J., "Characterization of nonlinear port parameters in loudspeaker modeling," in *Audio Engineering Society Convention 145*, New York City, 2018.

[13] "COMSOL Multiphysics v. 5.4," 2019.

[14] Bezzola, A., "Optimal Bass Reflex Loudspeaker Port Design," in *COMSOL Conference*, Boston, 2019.

[15] Brunet, P., "Use of repetitive multitone sequences to estimate nonlinear response of a loudspeaker to music," in *Audio Engineering Society Convention 143*, New York City, 2017.